Excerpt from the Proceedings of the 2011 COMSOL Conference in Boston

Patch Antenna Model for Unmanned Aerial Vehicle

Tom A. Eppes[*,1], Ivana Milanovic[1] and Sriramprasad Thiruvengadam[1]
[1]University of Hartford
*200 Bloomfield Ave., West Hartford, CT 06117, eppes@hartford.edu

Abstract: Patch antennas are widely used in communications links with unmanned aerial vehicles. Their hemispherical send and receive patterns enable the systems to maintain radio frequency contact over a wide range of vehicular attitudes. A microstrip-fed design offers other attractive features including lightweight, inexpensive, and a 3-D structure that can be easily integrated into the fuselage.

This paper describes the performance characteristics of a patch antenna for use in a 2.5 GHz band video downlink. The physical geometry, bandwidth, return loss, and near field patterns are discussed. The model uses COMSOL 4.2 and employs the electromagnetic module (emw) in stationary and parametric studies over a range of frequencies near 2.4GHz. The physical geometry of the antenna is 3-D and includes a coaxial input, microstrip feeder, rectangular patch, insulating dielectric and ground plane. A perfectly matched layer (PML) surrounds the antenna to improve the accuracy of the electromagnetic field solutions.

Keywords: patch antenna, electromagnetic fields, wireless communications.

1. Introduction

Patch antennas are widely used in communications links for applications where full duplex communications is required from one point to many points. In simplex systems where only one-way communications is needed, if the attitude of the transmitting antenna changes dynamically, the hemispherical radiation pattern afforded by a patch helps maintain the link. Such is the case with unmanned aerial vehicles with respect to their telemetry channels. A patch offers other attractive features including lightweight, inexpensive, and a thin structure that can be easily integrated onto the exterior skin of the vehicle. The beam half-width for a single rectangular patch is typically 20^o to 30^o which is acceptable considering the UAV attitude control capabilities.

This paper describes the performance characteristics of a patch antenna for use in a 2.4 GHz video downlink. The physical geometry, bandwidth, return loss, and near field patterns are discussed. The modeling process is similar to that described on the COMSOL website.[1]

The model employs the COMSOL 4.2 electromagnetic module (emw) in stationary and parametric studies over a range of frequencies. The 3-D geometry includes a coaxial input, microstrip feeder, metallic patch, insulating dielectric and ground plane. A perfectly matched layer (PML) hemisphere surrounding the antenna is used to improve accuracy.

2. Patch Antenna Design

The physical geometry of antenna is shown in Fig. 1. The 2.5 GHz input signal is fed from a 50 ohm coaxial cable that connects to the patch structure. The elements that compose this structure are a short microstrip feeder, active metallic patch area, insulating dielectric, and ground plane.

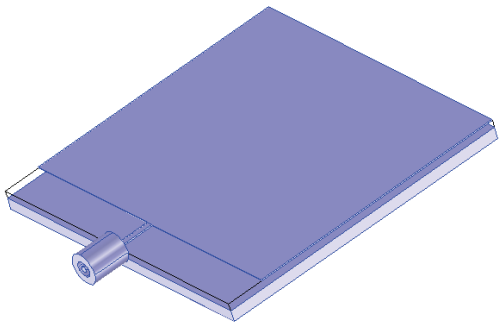

Figure 1. Patch antenna geometry.

The model contains three different materials, each with three properties, relative permittivity, relative permeability and electrical conductivity, set as shown in Table 1. The metal in both the inner and outer conductors of the coaxial cable as well as the patch assembly is assumed to be copper.

Table 1. Material properties.

Material	ε_r	μ_r	σ (S/m)
Copper	1.0	1.0	6e7
Mylar®	3.1	1.0	0.0
Air	1.0	1.0	0.0

For a single conducting strip located above one ground plane, the characteristic impedance, Z_0, is given by Eqn. 1.[2]

$$Z_0 = \frac{87}{\sqrt{\varepsilon_r + 1.41}} \ln\left(\frac{5.98h}{0.8w + t}\right) \quad (1$$

where Z_0 = characteristic impedance (ohms)
ε_r = relative permittivity of dielectric
h = thickness of dielectric layer (m)
w = conductor width (m)
t = conductor thickness (m)

A microstrip width of 1mm sets the above impedance at 50 ohms assuming a relative dielectric constant of 3.1 providing a good match to the coaxial cable.

Design of the active patch area proceeds as follows.[3-5] Starting with the center frequency, the wavelength in free space is

$$\lambda_0 = c/f_0 \quad (2$$

where c = 3e8 (m/s) = velocity of light in free space
f_0 = 2.5 (GHz) = center frequency

In this design, λ_0 turns out to be 12cm.

Both the microstrip, active patch area and ground plane are made from thin copper foil with a thickness of 127μm. The foil contains an adhesive backing so it can be pressed onto each side of the dielectric when the antenna is fabricated. A Mylar® layer of thickness, h, 0.75mm provides the dielectric boundary between the patch and ground plane layers. The width of the patch antenna, *W*, is computed as follows.

$$W = \frac{\lambda_0}{2}\left(\frac{\varepsilon_r + 1}{2}\right)^{-\frac{1}{2}} \quad (3$$

The next step is to compute the effective relative permittivity due to the presence of the dielectric.

$$\varepsilon_{eff} = \frac{\varepsilon_r + 1}{2} + \frac{\varepsilon_r - 1}{2}\left(1 + \frac{12h}{W}\right)^{-1/2} \quad (4$$

The effective length, L_{eff}, of the patch antenna is found by

$$L_{eff} = \frac{\lambda_0}{2\sqrt{\varepsilon_{eff}}} \quad (5$$

The length extension, Δl, is given by the following equation

$$\Delta l = 0.412h\left(\frac{\varepsilon_{eff} + .3}{\varepsilon_{eff} - .258}\right)\left(\frac{\frac{W}{h} + .264}{\frac{W}{h} + .8}\right) \quad (6$$

The length of the patch antenna is then the sum of the effective and extension lengths given by

$$L = L_{eff} + \Delta l \quad (7$$

In this design, the size of the active patch area is 4.27cm (width) by 3.46cm (length). The design did not include a quarter-wave impedance matching section before the patch. This would provide a better interface between the microstrip and patch offering a better return loss for the overall antenna.

3. Electromagnetic Equations

For a sinusoidal steady state solution, the governing equation for the electric field vector, **E**, is shown below.

$$\nabla \times \mu_r^{-1}(\nabla \times \mathbf{E}) - k_0^2\left(\varepsilon_r - \frac{j\sigma}{\omega\varepsilon_0}\right)\mathbf{E} = 0 \quad (8$$

where $k_0 = \omega_0\sqrt{\varepsilon_0\mu_0}$ = free space wave no.
$\omega_0 = 2\pi f_0$ (rad/s) = angular frequency
ε_r = relative permittivity of medium
ε_0 = permittivity of free space (farad/m)
μ_0 = permeability of free space (henry/m)
σ = electrical conductivity (S/m)

Several boundaries conditions are employed in the model. The PML boundaries are set to perfect electric conductors in which **n x E** = 0. The coaxial input is set to a lumped port condition at 10 volts. All copper surfaces are set

to an impedance boundary condition governed by the following equation.

$$\sqrt{\frac{\mu_0\mu_r}{\varepsilon_0\varepsilon_r - j\frac{\sigma}{\omega}}}\,\mathbf{n}\times\mathbf{H} + \mathbf{E} - (\mathbf{n}\cdot\mathbf{E})\mathbf{n} = (\mathbf{n}\cdot\mathbf{E}_s)\mathbf{n} - \mathbf{E}_s \quad (9$$

where **n** = unit vector normal to boundary
$\mathbf{E}_s$ = source electric field (V/m)
E = electric field (volt/m)
H = magnetic field (ampere/m)

4. Meshed geometry

A predefined mesh set to normal is used for the patch assembly and surrounding air based on a free tetrahedral. A swept mesh with 6 layers is used in the PML layer which results in a total of 251,907 elements with 1,351,802 degrees of freedom as illustrated in Fig. 2. As expected with this mode of meshing, the heaviest concentration of elements is located in the air and dielectric regions near the copper radiating components

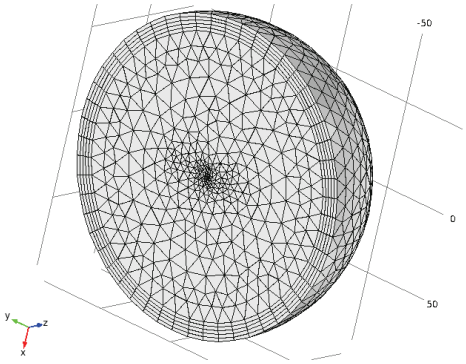

Figure 2. Meshed geometry.

5. Model Results

The first post-processing result in Fig. 3 shows a 3-D slice plot of the electric field 25mm above and parallel to the patch area. Even though it is a near field calculation, a relatively smooth distribution is observed.

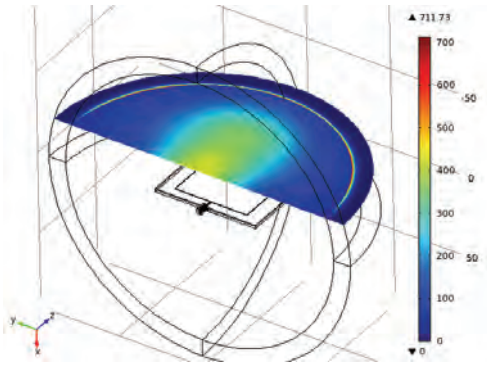

Figure 3. Electric field above patch.

Figure 4 shows the corresponding plot for the magnetic field in the same plane and 25mm offset distance above the patch. In this case, less symmetry is evident compared to the electric field. Not shown in Figs. 3 and 4, is the transition to more uniformity in both near fields as one moves farther from the active area.

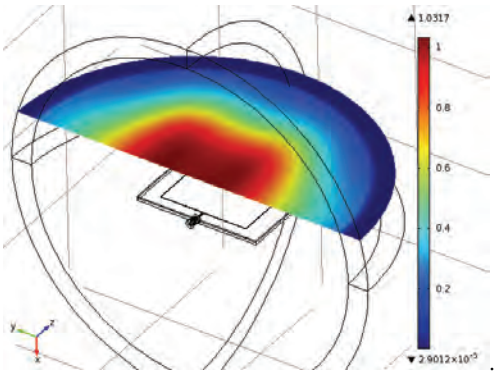

Figure 4. Magnetic field above patch.

Figure 5 is a 3-D arrow chart of average power flow in a slice plane mid-way along the antenna. As anticipated, strong radiating occurs vertically from the top of patch area.

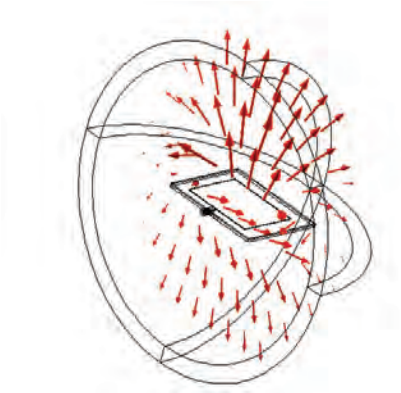

Figure 5. Average power flow above and below patch.

The next part of the study involves a parametric analysis 250 MHz above and below the operating frequency of 2.5 GHz. The return loss, S_{11}, in decibels is plotted in Fig. 6 and predicts -4dB at the operating frequency.

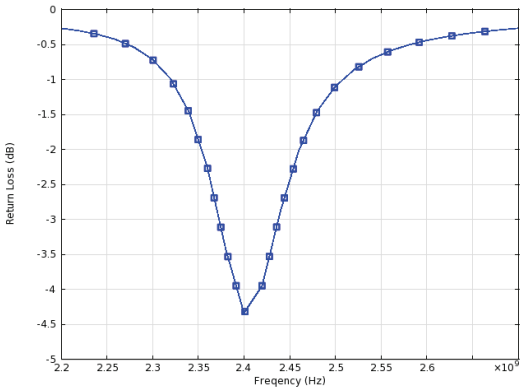

Figure 6. Return loss versus frequency.

6. Conclusion

This paper presents the results of an analysis of a patch antenna designed for use on a UAV. A 3-D model, developed in COMSOL 4.2 using the emw module, is the basis for the work. The electric and magnetic near fields along with the time average power flow are examined. In addition, a frequency sweep, near the operating frequency of 2.5 GHz estimates the return loss to be -4dB prior to employing any impedance matching techniques.

7. References

1. 'Balanced Patch Antenna for 6GHz,' http://www.comsol.com/showroom/downloadfile/model/782/version/comsol42/file/models.rf.patch_antenna.pdf, Accessed August 11, 2011.

2. Recht, E. and Shiran, S., "A Simple Model for Characteristic Impedance of Wide Microstrip Lines for Flexible PCB," *Proceedings of IEEE EMC Symposium 2000*, pp. 1010–1014.

3. Balanis, C., *Antenna Theory* (3rd Edition), Wiley 2005.

4. Johnson, R., *Antenna Engineering Handbook*, McGraw-Hill 1993.

5. Amman, M., "Design of Rectangular Microstrip Patch Antennas for the 2.4 GHz Band", Applied Microwave and Wireless, pp. 24 - 34, Nov/Dec 1997.